# Experimental and Evaluation of Flexural Capacity in Voided RC Slab with Internal Truncated Pyramid Shaped Voids

**Chatchawal Phuangruangsri* and Pornpen Limpaninlachat**

*Department of Civil and Environmental Engineering, Faculty of Engineering, Mahidol University, Nakhon Pathom, THAILAND*
**Corresponding author; E-mail address: chatchawal.phu@student.mahidol.ac.th*

## Abstract

Truncated Pyramid Shaped (TPS) voided former is an alternative voided shape embedded inside the reinforced concrete slab to reduce concrete quantity. The main purposes of this study were to investigate the one directional flexural behavior of TPS voided slab through the four-point bending test and compared the experimental results with the evaluation of flexural capacity. Two TPS voided slabs with dimension of 2700x1500 $mm^2$ and different thickness of 260 mm and 300 mm were subjected to the loading test. During the loading test, the results of load, deflection and strains in concrete and steel bars were recorded to observe their relevant behaviors. Consequently, the evaluation method for flexural capacity of the TPS voided slab was proposed by using the fundamental flexural analysis. Finally, the loading capacities from both specimens showed good agreement results between the experiment and evaluation method with an accuracy of up to 94.93%.

Keywords: Voided Slab, Truncated Pyramid Shaped Void, Flexural Bending Test, Evaluation of Flexural Capacity

## 1. Introduction

The voided slab is a type of reinforced concrete (RC) slab with air-space voids in the middle between upper and lower longitudinal steel bars inside the concrete. This system can reduce the concrete used with less environmental impact and more sustainability. In addition, the resistance of sound transmission and fire are also attained due to the air-filled insulation inside [1]. The reduction of concrete volume results in the overall structural weight and leads to a reduction in construction cost [2]. Some literatures stated that the self-weight of voided slab system can reduce up to 50% comparing with a conventional solid slab, while the flexural performance has been satisfied because the voids are in the non-critical section where is the tensile zone below the neutral axis [3-4]. Consequently, the longer span length can be designed resulting from obviously structural weight reduction [5].

Presently, there are many shapes of void formers such as spheres, ellipsoids, donuts, and truncated pyramids. The uses of spherical and ellipsoidal voids were first originated and have been used for a long time. From the design guideline for spherical and ellipsoidal voided slabs by Concrete Reinforcing Steel Institute (CRSI), there is a limitation of the depth of neutral axis of the voided slabs to not exceed 1.5 in or 3.8 cm to keep the rectangular shape of the compression zone, for an able the using design and analysis in the same principles as the conventional solid slab [6-7]. The void formers used in this study are Truncated Pyramid Shaped (TPS) voided formers that are made from recycled polypropylene. It has four conic-elevator feet to stand and fix the location inside the formwork. This type of void former can create the regular grid of orthogonal I-section lines at the solid section between two voids. This I-section will reduce more concrete weight than the other voided types and enhance the flexural performance resulting more cost-effective construction [8]. Moreover, the supported beams are unnecessary in this system because many orthogonal I-sections can transfer the structural load to the columns instead of beams [9].

Consequently, the main purposes of this study are to investigate the one-directional flexural behavior of TPS voided slab and to propose the evaluation method for predicting its flexural capacity. The voided slabs sized 2700x1500 $mm^2$ with different thickness and void-former sizes were subjected to the four-point bending test. Their flexural behaviors were observed through the experimental results such as the load—deflection

relationship and the several strains at concrete and steel reinforcing bars. The flexural capacities from experiments were collected and used for comparing with the proposed method to evaluate the flexural capacity by fundamental analysis.

## 2. Methodology and Materials

### *2.1 Details of experimental specimens*

To study the flexural behavior of TPS voided slab, the four-point loading test of full-scale one-way TPS voided slabs were conducted. The two experimental specimens defined as VS260 and VS300 had the same width and length of 1500 mm and 2700 mm. The depths of specimens were varied from 260 mm to 300 mm with two different heights of embedded TPS formers as 160 mm and 200 mm, respectively. The 16-mm diameter of deformed bars with 200-mm spacing were reinforced along the longitudinal direction of slab to resist bending force. Each slab contained eight TPS voided formers with the shortest spacing between the voids 90 mm, and the covering was 50 mm at the top and bottom of void. The 4 mm diameter of wire mesh with 200 mm of spacing were placed on the top of TPS voids to facilitate the force distribution from the loading plate and to prevent the temperature crack on the slabs. The shape of TPS void formers is shown in Fig.1. The details of V260 and V300 voided slabs are presented in Fig. 2 and Fig. 3, respectively.

### *2.2 Material properties*

#### *2.2.1 Concrete*

The designed cylindrical compressive strength of concrete was 32 MPa in the study. The ready-mix concrete was used for casting the large scale of slabs. The mix had the water-cement ratio of 0.5, and the targeted slump was 15-20 mm to obtain the sufficient strength and workability for construction.

#### *2.2.2 Reinforcing steel bars*

Eight deformed steel bars with diameter of 16 mm were used for longitudinal reinforcement. These bars were the grade of SD40 conformed to TIS 24-2016 [10], which had the yield and ultimate strength at least 390 MPa and 560 MPa, respectively. The properties of steel are shown in Table 1

#### *2.2.3 Truncated pyramid shaped void formers*

The void formers are made from polypropylene with truncated pyramid shapes. To control the depth of covering, the conic-elevator feet with 50 mm length were applied under the TPS void as shown in Fig. 1. In this study, two sizes of TPS void formers were used which were the height of 160 mm and 200 mm. These voided formers had the same top width and bottom width of 470 mm and 520 mm, respectively. The details of void formers are shown in Fig. 1 and Table 2.


**Fig. 1** TPS void former

**Table 1** Properties of steels

| Deformed steel bars | | Unit |
|---|---|---|
| Grade | SD40 | - |
| Yield strength | 390 | MPa |
| Tensile strength | 560 | MPa |
| Nominal area | 201.1 | $mm^3$ |

**Table 2** Details of void formers

| Parameter | VS260 | VS300 | Unit |
|---|---|---|---|
| Height | 160 | 200 | mm |
| Hollow space volume | 0.0031 | 0.0039 | $m^3$/pcs |
| Top area | 470x470 | 470x470 | $mm^2$ |
| Bottom area | 520x520 | 520x520 | $mm^2$ |
| Elevator foot height | 50 | 50 | mm |

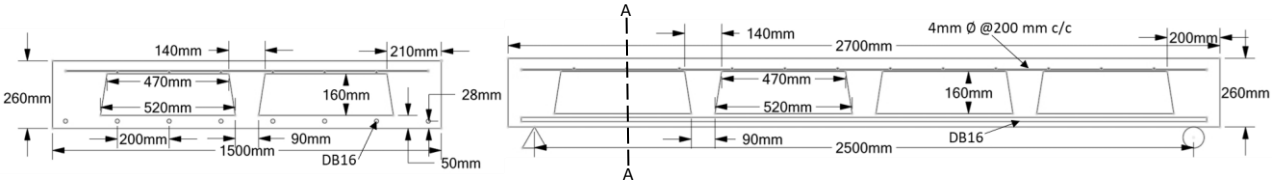


(a) A-A section (b) Longitudinal plane of voided slab

**Fig. 2** Details of VS260 specimen

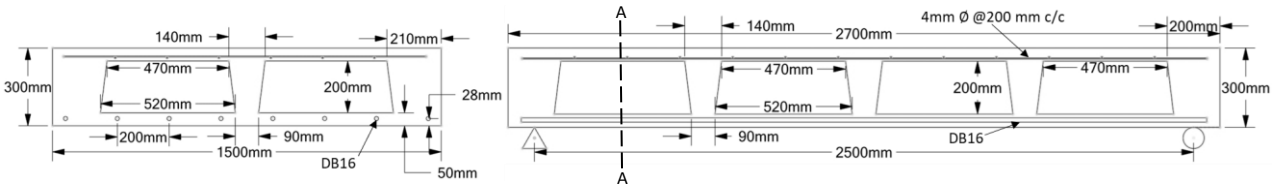


(a) A-A section (b) Longitudinal plane of voided slab

**Fig. 3** Details of VS300 specimen

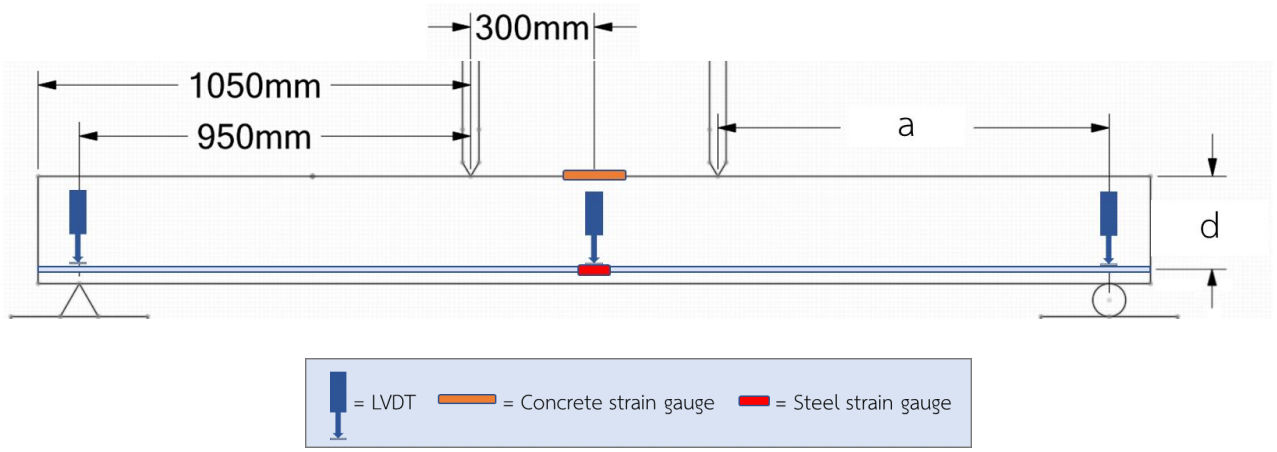


**Fig. 4** Locations of measuring instruments

*2.3 Experiment setup*

*2.3.1 Fabrication procedure*

Ready-mix concrete from the same batch was used for casting the voided slabs and cylindrical concrete for compression test. The slab formwork was installed from the steel and the black film-faced plywood. The longitudinal reinforcing steel bars (8DB16) were placed inside the steel formwork. Four strain gauges were attached on the steel reinforcing bars at the middle of slab to detect the real strain during the load test. Then, TPS void formers were placed, and followed by the placing of 4 mm diameter wire mesh above the void formers. The pouring process of concrete was divided into 2 layers, the first layer of concrete was poured until the level of the bottom voids, which equaled to height of elevator foot. The first layer was left for 45 minutes until the concrete paste became semi-fluid to prevent the floatation of void formers as shows in Fig. 5. The second ready-mix concrete was cast for the second layer until full depth of the slab. Additional concrete cylinder sized 100x200 mm and the concrete cylinder sized 150x300 mm were used to prepare specimens for conducting the compressive and tensile strength tests. One day after casting procedure, the steel formwork was removed, and continued curing process under moisture controlling by using a concrete curing agent and sack covering for 7 days. This further curing condition was simulated as the same at site construction.

(a) Before casting (b) After the first layer casting

**Fig. 5** Fabrication procedure

*2.3.2 Testing and instrumental setup*

The flexural behavior was investigated by four-point bending test. The one-way TPS voided slabs were subjected to a loading test with a span length of 2500 mm, the distance between the loading and supporting points was 950 mm. The two loading points were spanned with 300 mm apart from the center of slab as shown in Fig. 4. The *a/d* ratio was designed to be in the range of 2.5-6 which is the range for an intermediate-length beam and expected for flexural failure [11]. The Linear Variable Differential Transducer (LVDT) and strain gauges were used for measuring the real-time displacement and strains on the concrete and steel bars. The two 100-mm LVDTs were used to measure the average deflection at the mid-span, while the other two 50-mm LVDTs were used to measure the deflection at supports. The results from four LVDTs were applied for computing the relative deflection. To observe the behavior in concrete and steel bars,

the concrete strain gauges were used to measure the strain at the center on the top surface, and the steel strain gauges were used to measure strain at the center of the steel bars. The location of strain gauges on concrete and steel bars are shown in Fig. 7. The locations of measuring instruments are shown in Fig. 4. The load was applied by the 1000kN loading machine until failure of specimen. All experimental results were recorded by using data logger. The failure mechanism of the TPS voided slabs were observed and captured every 10 kN until failure.

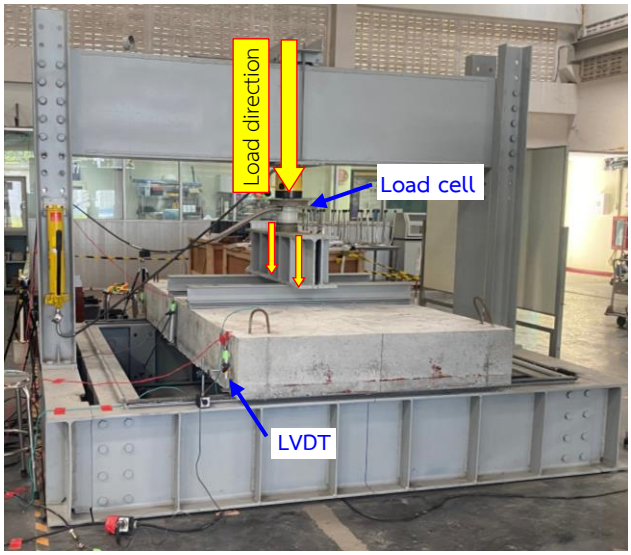


**Fig. 6** Four-point bending test of TPS voided slab

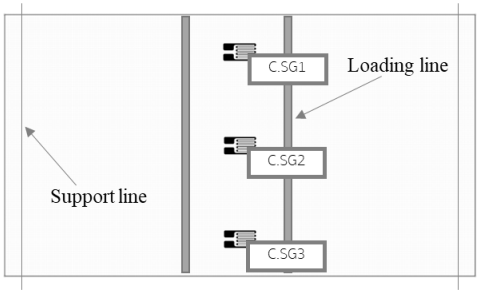


(a) On concrete

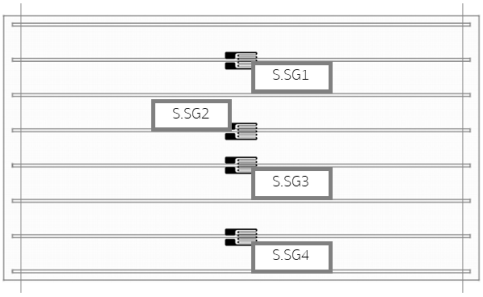


(b) On steel bars

**Fig. 7** Locations of strain gauges

## 3. Four-point bending test

### *3.1 Load—deflection behavior*

Figures 8(a) and 9(a) show the load versus relative deflection of the VS260 and VS300 under flexure. The two specimens had similar behaviors and failure pattern. When the initial load was applied to specimens, the load increased linearly until the point of first cracking load, which the flexural crack occurred from the bottom of the slab between two loading points region. After that, the load was increased with lesser slope of load—deflection relationship, this referred to the less stiffness of the slab due to several crack initiation and propagation. Moreover, the crack propagation and crack width had a possibility to be developed from the bottom of the slabs and through each reinforcing steel bar at different times, which might result in a small difference in the behavior of steel strain. The slope was reduced again when reaching the yield point. The yield point was defined as the strain on longitudinal steel bars yielded as shown in Fig. 8(b) and 9(b), which was the loading point at the first steel strain reached 0.002 mm/mm. The load was slightly increased and stabled after yielding steel initiation. Finally, the load reached the ultimate strength and suddenly dropped. The stiffness of VS300 is obviously higher than VS260 because of the thicker slab depth and the thicker voided slab also had the higher slope of first linear elasticity, then the slope gradually decreased in both specimens, this indicates that the flexural behaviors of TPS voided slabs have a possibility to use the same mechanism analysis as the conventional solid slab. The results from the experiment are summarized in Table 3.

### *3.2 Crack pattern*

Figures 11 and 12 show the crack pattern of VS260 and VS300 specimens. After the tensile stress exceeded the tensile strength of the concrete, the flexural crack occurred from the bottom edge of the concrete and developed toward the loading point. After this point, the flexural crack was widened with the load increasing, which related to the stiffness reduction in the load—deflection curve in previous section. Until the load at the yielding point, the crack had developed longer through the middle of the thickness relative to the yielding load as shown in Fig. 11(a) and 11(b). After yielding of steel bars, the flexural crack was continually widened. Finally, when the load reached

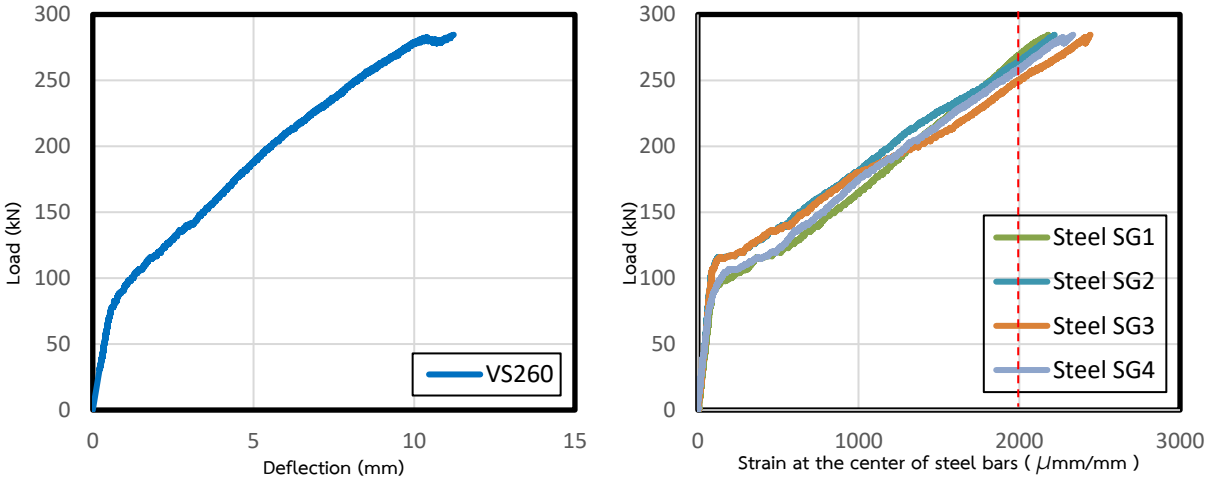


(a) Load—deflection curve (b) Load—steel strain curve

**Fig. 8** Experimental results of VS260

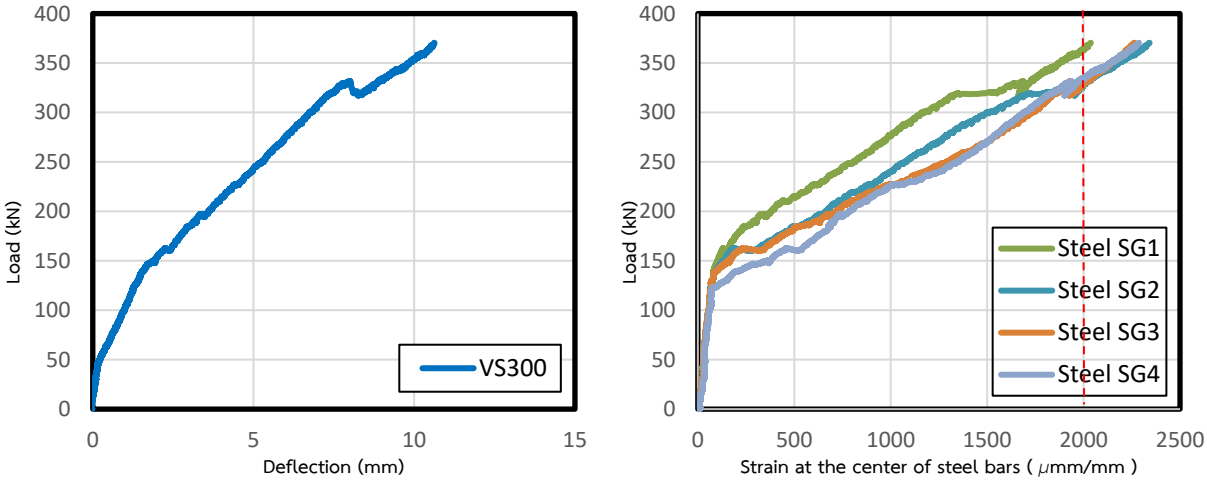


(a) Load—deflection curve (b) Load—steel strain curve

**Fig. 9** Experimental results of VS300

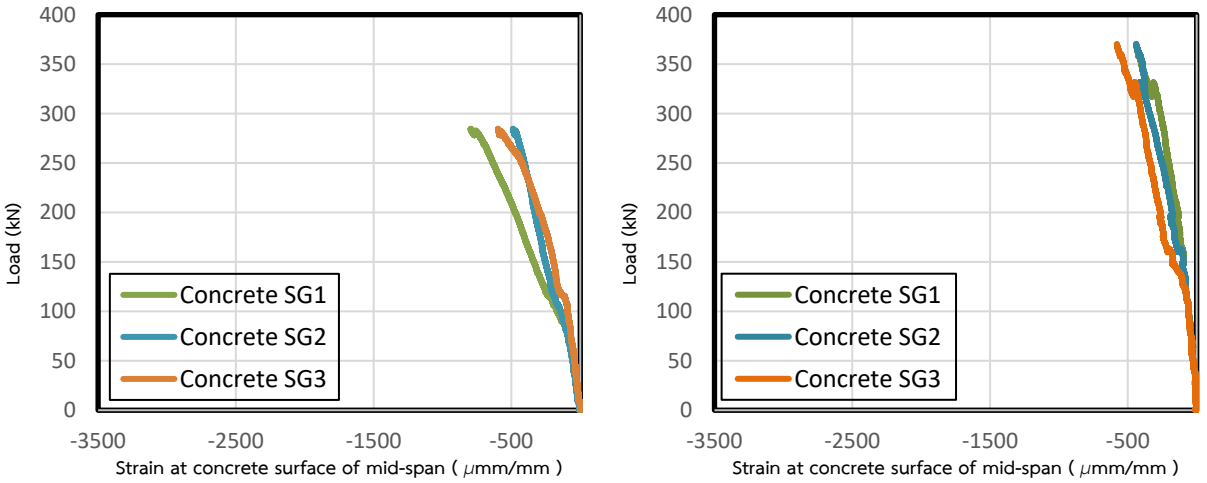


(a) VS260 (b) VS300

**Fig. 10** Load—strain curve at the concrete surface of VS260 and VS300

ultimate strength, the shear crack was suddenly occurred at the shear span as shown in Fig. 11(c) and 12, and the load immediately dropped. At this point, the compression strain on the top slab surface did not yield the ultimate concrete strain at 0.003 mm/mm.

From the resemble failure patterns and load—deflection relationship of these two specimens, it was noticed that even though the *a/d* ratio of the specimens was within the range of flexural failure, but the shear crack could be happened because no shear reinforcement was applied in this study, and the use of voided slab resulted in a significant loss of cross-sectional area to resist the one-way shear strength. However, all steel reinforcing bars has already yielded before the ultimate strength, this failure mode can be defined as the flexure-shear failure.

(a) At the first observable crack (at 136 kN)

(b) At the yield point

(c) At the ultimate point

**Fig. 11** Crack pattern of VS260

**Fig. 12** Crack pattern of VS300

**Table 3** Experimental results

| Data | VS260 | VS300 |
|---|---|---|
| Load at First cracking (kN) | 85.65 | 144.65 |
| Load at yield strength (kN) | 250.67 | 328.31 |
| Load at ultimate strength (kN) | 284.63 | 370.51 |
| Failure mode | Flexure-shear failure | Flexure-shear failure |

## 4. Evaluation of flexural capacity

Figure 16 shows the steps of evaluation for flexural capacity. In the case of VS260 and VS300 specimens, the neutral axis was fallen into the void's region, therefore the compressive area was not behaving like a rectangular shape but behaved like contiguous T-shapes due to the internal void formers. The evaluation began with the assumption of a neutral axis. The strain at each component along the cross-section was computed based on the remain-plan assumption. Therefore, each strain components were computed from the distribution diagram as shown in Fig. 13 with additional assumption of yielding strain in longitudinal steel bars as 0.002 mm/mm based on yield strength of the steel graded 390 MPa [12]. By assuming the yield strain at steel bars, the other strain components could be calculated accordingly. After that, the stresses of each component were investigated.

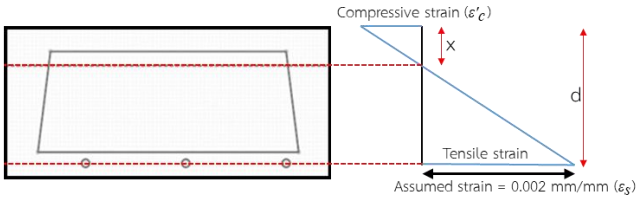


**Fig. 13** Strain distribution diagram

In case of concrete, the compressive strain along the cross-section was translated to the stress through the concrete's stress-strain model. To compute the flexural capacity of the TPS voided slabs, the evaluation of flexural capacity through fundamental analysis using the stress and strain model of concrete from Thorenfeldt [13] was proposed. The concrete model is shown in Fig. 14 and computed by using Eq. (1) to Eq. (4).

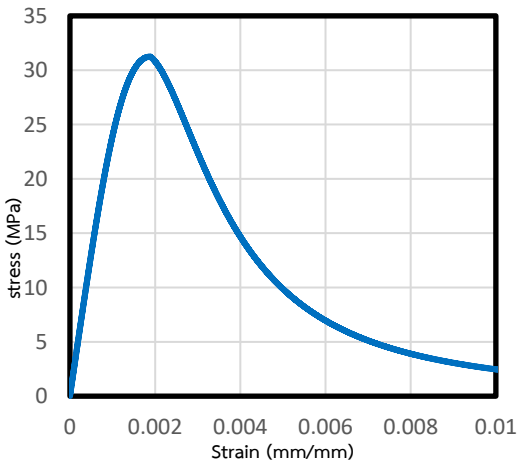


**Fig. 14** Compressive stress-strain model for $f_c' = 31.25$ MPa

$$\sigma'_c = \left[\frac{n(\varepsilon'_c/\varepsilon'_p)}{n\text{-}1+(\varepsilon'_c/\varepsilon'_p)^{nk}}\right] f'_c \quad (1)$$

$$n = 0.8+\frac{f'_c}{17} \quad (2)$$

$$k = \begin{cases} 1 & (0\le\varepsilon'_c\le\varepsilon'_p) \\ 0.67+\frac{f'_c}{62} & (\varepsilon'_c>\varepsilon'_p) \end{cases} \quad (3)$$

$$\varepsilon'_p = \frac{n}{n\text{-}1}\frac{f'_c}{1000E_c} \quad (4)$$

Where $f'_c$ is the compressive strength of concrete in MPa, $\sigma'_c$ is a concrete compressive stress in MPa, $\varepsilon'_c$ is a concrete compressive strain in mm/mm, $\varepsilon'_p$ is the concrete compressive strain at peak in mm/mm, and $E_c$ is Young's modulus of concrete in GPa.

According to the compressive strength test of cylindrical concrete, the average concrete compressive strength was equal to 31.25 MPa, which was used as the compressive strength for flexural calculation of VS260 and VS300 specimen. The compression force was computed using Eq. (5) to Eq. (6), $C$ is compression force in N, $A_c$ is compression area in mm.

$$C = \sigma'_c \times A_c \quad (5)$$

$$A_c = \begin{cases} b \times x & \text{(N.A. < covering)} \\ (b \times x)\text{-}2\left[\frac{(b_1+b_2)\times(x\text{-covering})}{2}\right] & \text{(N.A. > covering)} \end{cases} \quad (6)$$

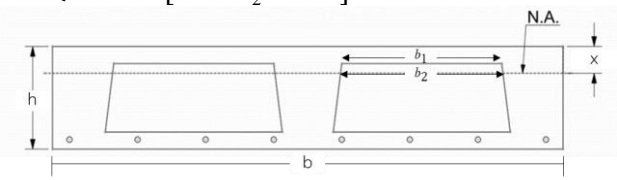


**Fig. 15** Meanings of parameters

Finally, the actual compression and tension force from the stress would be verified using the equilibrium equation. In the case of the forces were not equilibrium, the neutral axis would be assumed again, then the flexural capacity can be evaluated.

**Table 4** Summary of evaluation of flexural capacity

| Parameters | | VS260 | VS300 |
|---|---|---|---|
| Neutral axis (mm) | | 63.58 | 74.48 |
| Load at yield strength (kN) | Experiment | 250.67 | 328.31 |
| | Evaluation | 270.51 | 312.48 |
| Experiment/Calculation | | 0.93 | 1.05 |
| Accuracy (%) | | 92.66 | 94.93 |

Table 4 shows the comparison between the results from the experiment and the theory by evaluation. The ratios between experimental and evaluation results were equal to 0.93 to 1.05 which could be computed to the accuracy of 92.66 to 94.93%.

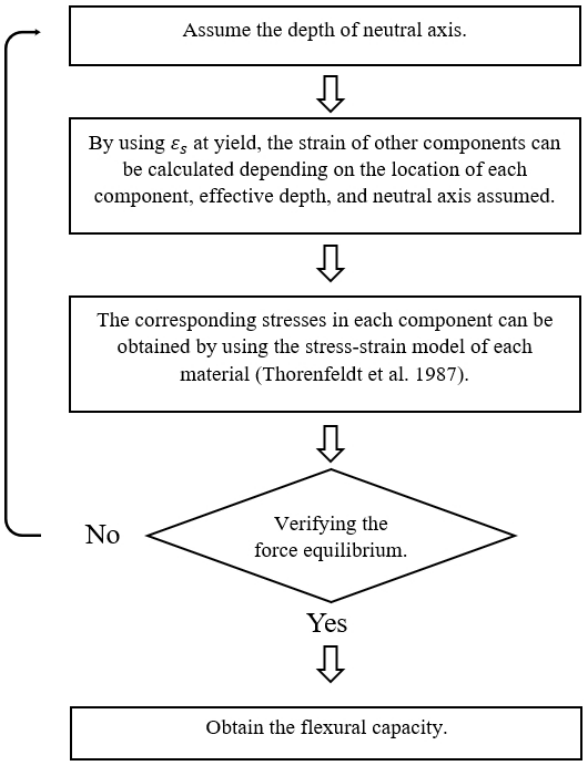


**Fig. 16** Calculating steps for flexural capacity

## 5. Conclusions

1. The failure pattern of flexural behaviors of the one-way TPS voided slabs were similar to the conventional solid slabs.

2. By increasing the thickness of TPS voided slab, the higher stiffness and flexural capacity can be achieved.

3. The comprehensive consideration for shear contributed by concrete should be considered with the effect of air-filled area instead of the concrete.

4. The conventional flexural analysis with the actual critical cross-section area in compression zone and using the concrete's stress-strain relationship can provide good prediction of flexural capacity of TPS voided slab.

## Acknowledgement

The authors would like to thank Kor-IT Design and Construction Company Limited for the facilitation of the resource and equipment to conduct in this study.

## References

[1] Taslim, S. (2020) A review paper on "U-Boot Beton: The concrete saver". *International Journal of Scientific and Research Publications*, 10(7), pp. 756-757.

[2] Anil, A., & Jose, V. (2020). Review on U Boot technology in construction. *International Journal of Engineering Trends and Applications*, 7(6), pp. 6-9.

[3] Harding, P. (2004) BubbleDeck advanced structure engineering. *BubbleDeck Artic*, pp. 15–16.

[4] Gamal, M., Heiza, K., Hekal, G. M., & Nabil, A. (2023). Voided slabs as a new construction technology-a review. *International Conference on Advances in Structural and Geotechnical Engineering*, Hurghada, Egypt, 6-9 March 2023.

[5] International Federation for Structural Concrete (fib). (2005). Post-tensioning in buildings. *Fib-Bulletin No. 31*. Case Postal 88, CH-1015 Lausanne, Switzerland.

[6] Concrete Reinforcing Steel Institute. (2014). *Addendum – Design Guide for Voided Concrete Slabs*. 933 N. Plum Grove Rd. Schaumburg, USA.

[7] Wheeler, H. (2018). *Flat Plate Voided Slabs: A Lightweight Concrete Floor System Alternative*. Department of Architectural Engineering, Kansas State University, Manhattan, Kansas.

[8] Taskin, K., & Peker, K. (2014). Design factors and the economical application of spherical type voids in RC slabs. *Proceedings of International Scientific Conference People, Buildings and Environment*, pp. 448-458.

[9] Daliform Group. (2014). *U-Boot Beton System Study: Lightened Concrete Slab by using U-Boot Beton*. Gorgo al Monticano, Treviso, Italy.

[10] Thai Industrial Standards Institute. (2016). *TIS 24-2548: Steel Bars for Reinforced Concrete: Deformed Bars*. 75/42 Rama VI Road, Ratchathewi, Bangkok, Thailand.

[11] Wang, C. K., Salmon, C. G., Pincheira, J. A. (2006). *Reinforced concrete design*. University of Wisconsin Maddison.

[12] ACI Committee 318. (2019). *Building Code Requirements for Structural Concrete*. American Concrete Institute 38800 country club drive, Farmington Hills, MI, USA.

[13] Thorenfeldt, E., Tomaszewicz, A., and Jensen, J. J. (1987). Mechanical properties of High strength concrete and application in design. *Proceedings of the Symposium Utilization of High-Strength Concrete*, Tapir, Trondheim, pp. 149-159.